Applied Physics B (2024) 130:9
https://doi.org/10.1007/s00340-023-08151-3

Applied Physics B
Lasers and Optics

RESEARCH

Determination of the effective optical path length of integrating cavity by measuring emitted light

Zhiyang Sun[1] · Yongda Wang[1] · Rui Zhang[1] · Zhiguo Zhang[1,2]

Received: 27 July 2023 / Accepted: 23 November 2023 / Published online: 13 December 2023
© The Author(s), under exclusive licence to Springer-Verlag GmbH Germany, part of Springer Nature 2023

Abstract

The port fraction in an integrating cavity is defined as the ratio of the area of all the leaky ports to the total internal surface area of the cavity. It allows for the regulation of the cavity's output radiation flux, thereby influencing the formed light field within the cavity. Building upon this fundamental parameter, we present a technique for determining the effective optical path length (EOPL) of an integrating cavity by examining the output light's variation as a function of port fraction. A relationship between the EOPL and cavity parameters has been established without the presence of gas absorption. To corroborate the method, we calculated the EOPL of the cavity at 764 nm employing both our proposed method and the gas absorption-based approach. Upon comparison, it was observed that the two methods yielded consistent EOPL results, specifically 109.5 (2) cm and 109 (2) cm, respectively. This study demonstrates that the output light from an integrating cavity indeed conveys information about its EOPL in the absence of gas absorption. This insight holds significant value for determining the EOPL of integrating cavities as well as other optical cavity types.

1 Introduction

Gas composition analysis plays a crucial role in a myriad of scientific and industrial applications, including atmospheric component analysis [1], breath diagnostics [2], and oil refining [3]. Over the years, a multitude of approaches have been developed to achieve precise and sensitive gas detection [4, 5]. For small molecule gases with narrow absorption peaks, such as methane, oxygen, and nitric oxide, laser absorption spectroscopy is often employed [6–8]. In pursuit of enhanced sensitivity, several laser-based gas detection techniques have been proposed, including tunable diode laser absorption spectroscopy (TDLAS) [9], photoacoustic spectroscopy (PAS) [10], and cavity ring-down spectroscopy (CRDS) [11]. Nonetheless, these laser-based methods face challenges in analyzing multi-component gases containing larger molecules, as the broad absorption peaks of large molecules and overlapping absorption peaks among different gases hinder accurate detection. In contrast, incoherent light-based Fourier transform spectroscopy (FTS) is typically used for the analysis of multi-component gases containing larger molecules such as sulfur hexafluoride [12], ethane [13], propane [14], and carbon dioxide [15]. Despite its advantages, achieving sensitive detection of multi-component gases containing large molecules using FTS remains a formidable challenge due to the limited optical path length inherent to the technique.

According to the Beer–Lambert law, one direct and effective approach to enhance gas detection sensitivity is to increase the optical path length [16, 17]. Over the past several decades, substantial research has been devoted to achieving this aim. For non-coherent light, integrating cavities are commonly employed as gas cells to amplify the effective optical path length (EOPL), including integrating spheres [18] and cubic integrating cavities (CIC) [19]. Gao et al. proposed a method to ascertain the EOPL of an integrating sphere by contrasting the absorption signal of oxygen within the cavity to that in the air, employing the TDLAS technique. This approach allows for the determination of the EOPL of an irregularly shaped integrating cavity without requiring the cavity's parameters [20]. In comparison to gas absorption-based EOPL measurement methods, Zhou et al. demonstrated a EOPL measurement technique for integrating cavity based on the time-resolved spectroscopy [21]. The method, which does not rely on the presence

✉ Zhiguo Zhang
zhangzhiguo@hit.edu.cn

[1] School of Instrumentation Science and Engineering, Harbin Institute of Technology, Harbin 150001, China

[2] School of Physics, Harbin Institute of Technology, Harbin 150001, China

of gas absorption, can derive the EOPL by multiplying the cavity's time constant τ with the speed of light c. Intriguingly, in the absence of gas absorption, the light emitted from the integrating cavity is associated with the multiple diffuse reflection processes the light undergoes within the cavity. Consequently, the emitted light inherently contains information about the EOPL of the cavity. However, to date, the exploration of the relationship between the EOPL of the cavity and its emitted light in the absence of gas absorption remains limited.

In this letter, we introduce a method for determining the EOPL of an integrating cavity by analyzing the variation in the output light from the cavity in relation to the port fraction. We establish the relationship between the EOPL and the parameters of the integrating cavity in the absence of gas absorption. To validate the proposed method, we compared the EOPL results derived from our method with those obtained through a gas absorption-based method at the same wavelength. Lastly, we employed our proposed method to determine the EOPL of the cavity across five distinct wavelengths.

2 Theory

For an arbitrary-shaped integrating cavity, as long as a uniform light field distribution can be formed rapidly after the light enters the cavity, its EOPL, L_{eff}, can be expressed as [22]:

$$L_{eff} = L_0 + \frac{L_{ave}}{1 - \rho(1 - f_0)}. \tag{1}$$

where, L_0 is additional path length which depends on the specific launch and delaunch conditions [23]. L_{ave} is the single-pass average path length, which equals to 4 V/S (V and S are the volume and the inner surface area of the cavity, respectively). ρ is the diffuse reflectance. f_0 represents the initial port fraction, which is determined by the sum of initial port areas divided by the total inner surface area of the cavity. Given that the diffuse reflectance ρ is wavelength-dependent, the EOPL L_{eff} consequently varies with the wavelength.

In Eq. (1), we can calculate the EOPL if we know the values of the additional path length L_0, the single-pass average path length L_{ave}, the reflectance ρ, and the initial port fraction f_0. Generally, it is relatively simple to determine the values of L_0 and L_{ave}. The additional path length, L_0, can be determined based on the incident light conditions, while the single-pass average path length, L_{ave}, can be derived from the volume V and surface area S of the cavity. Therefore, determining L_{eff} can be accomplished once the remaining two parameters, ρ and f_0, are obtained. In cases where no gas absorption is present within the cavity, the relationship between the incident and emitted radiant flux of the cavity can be expressed as follows:

$$\Phi = \frac{f_{out}}{1/\rho - (1 - f)} \Phi_0, \tag{2}$$

where, Φ is the emitted radiant flux, Φ_0 is the incident radiant flux, f_{out} is the port fraction of the output aperture. f is the total port fraction. In general, the port fraction of an integrating cavity is difficult to change continuously and is usually obtained by measuring the size of the cavity's apertures. Therefore, in most cases, the port fraction is considered to be a constant rather than an independent variable. Here, we introduce an additional port fraction (APF) f_x and treat it as a variable in order to observe the effect of the port fraction on the other parameters of the cavity and attempt to derive these parameters from the relationship. The APF is defined as the ratio of the area of the additional port to the total internal surface area of the cavity. It allows for the regulation of the cavity's output radiation flux, thereby influencing the formed light field within the cavity. By expressing f as the sum of f_0 and f_x, Eq. (2) can be further written as:

$$\Phi = \frac{f_{out}}{1/\rho - (1 - f_0 - f_x)} \Phi_0. \tag{3}$$

According to Eq. (3), we can measure the emitted radiant flux Φ at single wavelength while varying the APF, f_x, treating other parameters in Eq. (3) as constants. In this way, we can determine the parameters ρ and f_0 by performing the Least Squares fitting on the acquired data. The value of L_{eff} can be obtained by substituting the values of ρ and f_0 into Eq. (1). As we are aware, adjusting the aperture size of an integrating sphere continuously can be challenging. Therefore, we have chosen to use a CIC for subsequent experiments to validate our idea, as its port fraction can be easily adjusted by simply moving the top lid of the cavity. In these experiments, multiple lasers with specific wavelengths of 405, 450, 520, 650, 764 and 785 nm were employed.

3 Experiments

The schematic diagram of the experimental setup is shown in Fig. 1. An 8 cm CIC, crafted from black polymethylmethacrylate and featuring a movable lid, was employed for the validation. The inner surface of the cavity was coated with a barium sulfate-based material (Avian Technologies, Avian-D) [24] with the aim of approximating the properties of an ideal Lambertian reflector. The light beam emitted by the laser diode, modulated by a sawtooth wave, is introduced into the cavity through the input aperture. The light beam undergoes diffuse reflections within the cavity before

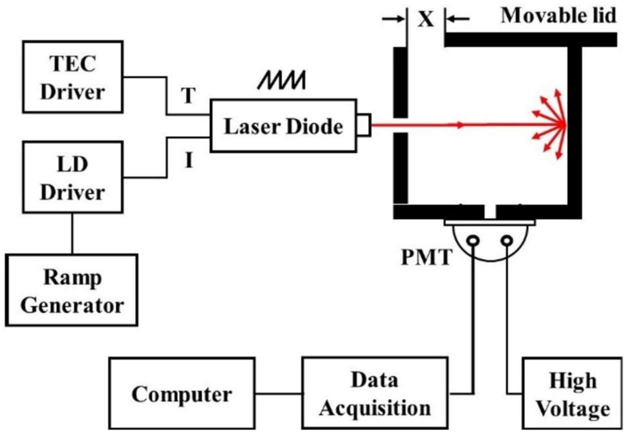

Fig. 1 Schematic of experimental setup for determination of EOPL using a CIC. Multiple lasers of different wavelengths were employed, although only one is shown for clarity

exiting through the output aperture, where it is detected by a photomultiplier tube (Zolix Instruments, CR131). During the experiment, the port fraction is modified by adjusting the position of the cavity lid. Importantly, this adjustment does not impact the integrity of the coating and structure of the CIC. For further details on this point, please refer to the supplementary material. The emitted radiant flux, corresponding to various port fractions, is recorded using a data acquisition card (Zolix Instruments, DCS103). To precisely control the output of the laser, laser diodes were affixed to a thermo-electrically cooled base (Thorlabs, TCLDM9). The temperature and current of these laser diodes were regulated using a temperature controller (Thorlabs, TED 200C, − 45 °C to + 145 °C, ± 0.01 °C) and a current controller (Thorlabs, LDC 205C, 0–500 mA, ± 0.1 mA), respectively. In the experiments, laser diodes were employed as light sources. These included lasers with specific wavelengths of 405 nm (Nichia, NDHV210), 450 nm (Sharp, GH04580A2G), 520 nm (Osram, PLT5), 650 nm (SHHO, SLD650005TN-A), 764 nm (Thorlabs, L763VH1) and 785 nm (Sharp, GH0782RA2C).

To make a comparison with the EOPL measurement method based on gas absorption, we decided to measure the EOPL of the CIC at 764 nm, a choice motivated by the known absorption properties of oxygen present in the air at this wavelength. However, it is necessary to perform the experiment under oxygen-free environment to measure the EOPL at 764 nm using our method. This typically requires time-consuming and cumbersome measures such as vacuum pumping or nitrogen purging of sealed chambers. To circumvent these steps while still employing our method to measure the EOPL of the CIC at 764 nm, we devised a strategy to conduct the experiment in the air: namely, using a waveform generator to modulate the output of the laser with a sawtooth wave, causing the laser wavelength to sweep across the

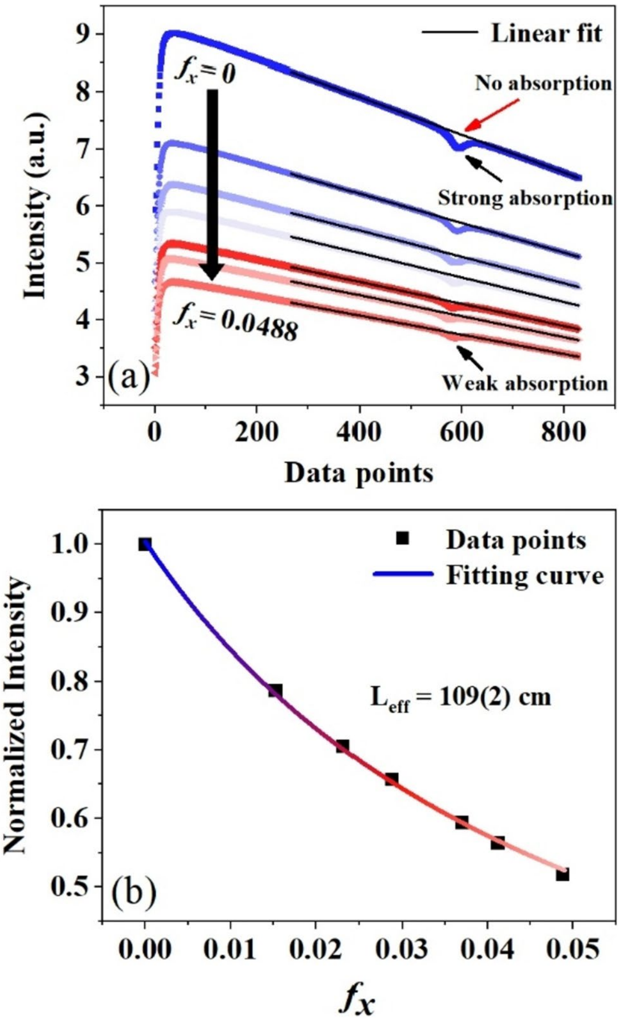

Fig. 2 **a** Variation of emitted light intensity after sawtooth wave modulation as a function of APF. The dips represent the absorption of oxygen in air. The fitting lines represent the emitted light intensity in the absence of oxygen. **b** The change in emitted light intensity at 764 nm represented by the fitting lines for the oxygen-free condition as a function of APF

oxygen absorption line in the air at 764 nm. By performing a linear fit on the modulated light emitted from the cavity, we were able to ascertain the intensity of light emitted from the cavity at 764 nm in the absence of oxygen absorption, as depicted in Fig. 2a.

4 Results and discussion

As shown in Fig. 2b, with the increase in the APF from 0 to 0.0488, the intensity of the modulated light emitted from the cavity is seen to decrease. The dips indicated by the black arrows correspond to the absorption of oxygen at 764 nm in the air. To obtain the output light intensity at 764 nm in the absence of oxygen, we used the value of the fitting line at the point (indicated by the red arrow) as the cavity output intensity at 764 nm under an oxygen-free environment. Through linear fitting of the emitted light corresponding to each APF, we obtain the relationship of the cavity's emitted light at 764 nm under oxygen-free conditions as a function of the APF, as depicted in Fig. 2b. Corresponding to the results depicted in Fig. 2a, the output light intensity is observed to gradually decrease as the APF increases. Utilizing Eq. (3), we have fitted the data points and subsequently determined the values of the fitting parameters ρ and f_0. Given that the theoretical relationship between the cavity's output light and the port fraction is known, typically, 3–5 data points are sufficient for fitting to determine values of ρ and f_0. However, to ensure a more precise fit, we employed between 7 to 9 data points in our study's fitting process. In light of the laser's trajectory from the cavity's entrance aperture to the point of its initial reflection, which precisely corresponds to the cavity's side length, values $L_0 = 8$ cm and $L_{ave} = 4$ V/S = 5.333 cm are obtained. Substituting these four parameters into Eq. (1) yields the EOPL of the cavity as 109(2) cm.

Subsequently, we employed a measurement method based on gas absorption to gauge the EOPL of the cavity at 764 nm. At room temperature and atmospheric pressure, the concentration of oxygen in air and its absorption cross-section at 764 nm remain constant. According to Beer-Lambert's law, there exists a direct proportionality between the optical path length of oxygen and its absorbance under these conditions. By measuring the absorbance of oxygen in air over varying lengths of optical paths, this linear relationship can be established. Utilizing this linear relationship, the EOPL within the CIC can be determined based on the absorbance of oxygen in the CIC. During the experiment, the movable lid was kept in a closed position. The CIC was filled with room air and was in communication with the atmosphere through the input and output apertures.

Specifically, we utilize the linear relationship between the optical parameter (OP), which is defined as the peak value of the absorbance, and the optical path length to determine the EOPL of the CIC. According to Beer–Lambert's law, the relationship between the outgoing light intensity and the incoming light intensity after passing through a gas medium is given by:

$$\Phi(v) = \Phi_0(v) \exp[\sigma(v)NL]. \tag{4}$$

Here, $\sigma(v)$ represents the absorption cross-section of the gas, N is the number density of the gas particles, and L is the optical path length. By rearranging the Eq. (4), we obtain:

$$A(v) = \ln \frac{\Phi_0(v)}{\Phi(v)} = \sigma(v)NL. \tag{5}$$

Here, $A(v)$ is the absorbance. OP is defined as the peak value of the absorbance, i.e.,

$$OP = A(v_0) = \ln \frac{\Phi_0(v_0)}{\Phi(v_0)}, \tag{6}$$

where v_0 is the frequency corresponding to the peak value of the absorbance.

The experimental results are presented in Fig. 3. The black data points represent the oxygen absorption corresponding to different optical path length in air, while the red data point represents the oxygen absorption corresponding to the EOPL within the CIC. The EOPL of the cavity was found to be 119.7 (2) cm. The inset in Fig. 3 is a magnified view at $L = 0$ cm, revealing that the optical parameter value does not equal zero when the optical path length $L = 0$ cm. This discrepancy is due to the hidden optical path contained in the measured optical path, which mainly includes the optical paths within the laser and detector where air is present. Therefore, the EOPL of the cavity should be corrected by subtracting this part, resulting in a true EOPL of 109.5 (2) cm. This value is consistent with the result obtained from the proposed method, indicating that both the absorption-based approach and the proposed method in this study are viable for determining the EOPL of an integrating cavity. While simulation-based approaches can be used to determine the EOPL of the integrating cavity, experimental methods remain a reliable and precise means for this determination. Typically, simulation-based determinations are considered only when experimental methods are not feasible.

Following this, we utilized the validated method to measure the EOPL of CIC at five different wavelengths within

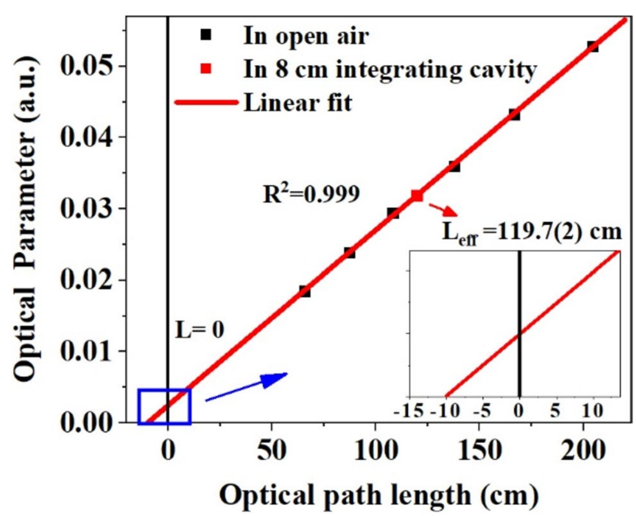

Fig. 3 Determination of EOPL of the CIC using a method based on gas absorption. The inset illustrates the intersection point of the fitting line and the coordinate axes when the optical path length $L = 0$ cm

the visible light range (405, 450, 520, 650, and 785 nm). Because in air, there's negligible gas absorption at these wavelengths, we're enabled to measure the variation of the emitted light as a function of APF in air using our method without necessitating laser modulation. The results are depicted in Fig. 4. It can be observed that the decrease in the emitted light intensity with increasing APF varies for different wavelengths, which is due to the wavelength-dependent diffuse reflectance. Moreover, the agreement between the points and the fitting curves for different wavelengths demonstrates the feasibility of using Eq. (3) to describe the relationship between the CIC emission and the port fraction. Further, we obtained the fitting parameters ρ and f_0 for the different wavelengths, yielding the EOPL of the cavity as 71(2) (405 nm), 84(2) (450 nm), 107(2) (520 nm), 125(2) (650 nm) and 115(2) cm (785 nm). For any subsequent experiments involving gas concentration measurements using the CIC, resealing the top cover of the cavity is a necessary step.

When employing the integrating cavity in conjunction with Fourier Transform Infrared Spectroscopy (FTIR) for multi-component gas concentration measurements, it's frequently encountered that both the composition and concentration of the target gas are indeterminate. This ambiguity poses challenges in accurately predicting the exact positions of the gas absorption peaks. Even when equipped with knowledge of a gas's absorption cross-section at various wavelengths, the concentration values derived from different absorption peaks of the same gas might still differ. This discrepancy is primarily due to the wavelength-sensitive nature of the EOPL within the cavity. Therefore, by preemptively determining the cavity's EOPL using our proposed method,

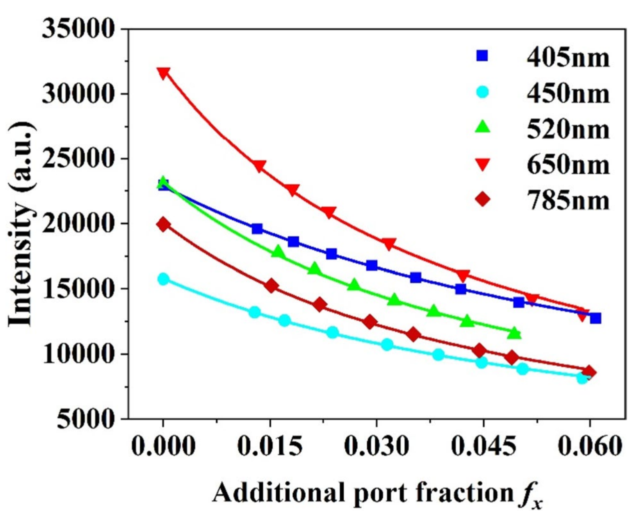

Fig. 4 The emitted light variation with APF and corresponding fitting curves at 405, 450, 520, 650 and 785 nm

we can effectively negate the interference caused by its wavelength-dependent variations during gas measurements.

Moreover, compared to the arduous and time-consuming task of utilizing absorption peaks from various possible gases to ascertain the EOPL of the cavity (the absorption-based approach), the method we proposed sidesteps the need for gas absorption within the cavity. As a result, our approach enables the use of broadband light sources, offering a straightforward means to garner comprehensive insights into the EOPL's variation with wavelength. This foundational work paves the way for precise measurements of multi-component gases through the synergistic use of integrating cavity and FTIR technologies.

5 Conclusions

In summary, a method for determining the effective optical path length of an integrating cavity by measuring the output light corresponding to different port fractions has been proposed. The relationship between the effective optical path length and the cavity parameters has been established in the absence of gas absorption. To validate our method, we determined the effective optical path length of the cavity at 764 nm using both a gas absorption-based method and the proposed method, finding a consistent outcome from both techniques. This research confirms that the output light from an integrating cavity inherently contains information about its EOPL when gas absorption is not a factor. This revelation is invaluable for ascertaining the EOPL of integrating cavities as well as other optical cavity configurations. In future work, we will explore the use of broadband light sources with the aim of obtaining comprehensive profiles of EOPL as a function of wavelength.

Supplementary Information The online version contains supplementary material available at https://doi.org/10.1007/s00340-023-08151-3.

Acknowledgements This work was supported by the National Key Research and Development Program of China (2016YFF0102803).

Author contributions Zhiyang Sun: Conceptualization, Methodology, Validation, Formal analysis, Investigation, Resources, Data curation, Writing- Original draft preparation. Yongda Wang: Validation, Data curation. Rui Zhang: Manuscript revision, Supervision. Zhiguo Zhang: Conceptualization, Methodology, Supervision.

Data availability Data underlying the results presented in this paper are not publicly available at this time but may be obtained from the authors upon reasonable request.

Declarations

Conflict of interest The authors declare that they have no known competing financial interests or personal relationships that could have appeared to influence the work reported in this paper.

References

1. Q. Zhang, T. Zhang, Y. Wei, T. Liu, Appl. Opt. **62**, 4409 (2023)
2. Z. Li, D. Jiang, M. Zhang, J. Li, Infrared Phys. Tech. **133**, 104815 (2023)
3. L. Weng, H. Wang, Q. Yang, J. Phys. Conf. Ser. **2464**, 012013 (2023)
4. J. Chang, Q. He, J. Li, Q. Feng, Microw. Opt. Technol. Lett.. Opt. Technol. Lett. **65**, 1141 (2023)
5. X. Zhou, Y. Tang, S. Zhao, H. Chen, H. Li, Optik **287**, 171126 (2023)
6. W. Ye, X. Xu, C. Peng, X. Xiao, Z. Xia, W. Liu, W. Luo, F. Wu, T. Wu, Microw. Opt. Technol. Lett.. Opt. Technol. Lett. **65**, 1031 (2023)
7. J. Chang, Q. He, M. Li, Sensors **23**, 4274 (2023)
8. J. Li, Y. Zhou, L. He, Z. Wang, W. Ma, Y. Ji, L. Song, Infrared Phys. Tech. **133**, 104813 (2023)
9. H. Cui, F. Wang, S. Hu, W. Wang, J. Fan, Instrum. Sci. Technol.. Sci. Technol. **51**(5), 544 (2023)
10. B. Li, H. Wu, C. Feng, S. Jia, L. Dong, Anal. Chem. **95**, 6138 (2023)
11. Q. Sun, M. Gu, D. Wu, T. Yang, H. Wang, Y. Pan, Atmos. Environ. **307**, 119848 (2023)
12. X. Zhang, H. Liu, J. Ren, J. Li, X. Li, Spectrochim. Acta Part A **136**, 884 (2015)
13. J.J. Harrison, N.D.C. Allen, P.F. Bernath, J. Quant. Spectrosc. Radiat. TransferSpectrosc. Radiat. Transfer **111**, 357 (2010)
14. C.A. Beale, R.J. Hargreaves, P.F. Bernath, J. Quant. Spectrosc. Radiat. TransferSpectrosc. Radiat. Transfer **182**, 219 (2016)
15. S.W. Bruun, A. Kohler, I. Adt, G.D. Sockalingum, M. Manfait, H. Martens, Appl. Spectrosc.Spectrosc. **60**, 1029 (2006)
16. D. Das, A.C. Wilson, Appl. Phys. B **103**, 749 (2011)
17. X. Liu, G. Gao, X. Yu, Z. Gao, T. Cai, Infrared Phys. Technol. **114**, 103654 (2021)
18. J. Hodgkinson, R.P. Tatam, Meas. Sci. Technol. **24**, 012004 (2012)
19. J. Yu, Q. Gao, Z. Zhang, Infrared Sens. Dev. Appl. IV, SPIE **9220**, 150 (2014)
20. Q. Gao, Y. Zhang, J. Yu, Z. Zhang, S. Wu, W. Guo, Appl. Phys. B **114**, 341 (2014)
21. X. Zhou, J. Yu, L. Wang, Z. Zhang, Appl. Opt. **57**, 3519 (2018)
22. X. Zhou, J. Yu, L. Wang, Z. Zhang, Appl. Sci. **8**, 1630 (2018)
23. J. Hodgkinson, D. Masiyano, R.P. Tatam, Appl. Opt. **48**, 5748 (2009)
24. A. Technologies, "Avian-d white reflectance coating," [EB/OL]. https://aviantechnologies.com/product/avian-d-white-reflectance-coating/. Accessed 1 May 2022

Publisher's Note Springer Nature remains neutral with regard to jurisdictional claims in published maps and institutional affiliations.

Springer Nature or its licensor (e.g. a society or other partner) holds exclusive rights to this article under a publishing agreement with the author(s) or other rightsholder(s); author self-archiving of the accepted manuscript version of this article is solely governed by the terms of such publishing agreement and applicable law.